2019 American Control Conference (ACC)
Philadelphia, PA, USA, July 10-12, 2019

Trajectory Tracking Control of a nonlinear Autonomous Surface Vessel

David Cabecinhas and Carlos Silvestre, *Member, IEEE*

***Abstract*— This paper presents a nonlinear controller based on a double integrator system for trajectory tracking of a nonlinear autonomous surface vessel. Using a fixed-point on the vessel body frame as position output, we devise a simplified controller with only two error states, as opposed to the four required in a more straightforward and naive backstepping approach. The resulting controller is dynamically simple and easy to implement, and does not require higher than second-order plant dynamics and reference trajectory derivatives. The proposed approach mitigates typical problems arising during backstepping such as noise amplification and the need for a highly accurate plant model. Experimental results with an instrumented autonomous surface vessel are presented to corroborate the performance and robustness of the proposed controller.**

I. Introduction

Recent technological developments have propelled autonomous marine vehicles to play an ever-increasing role in the analysis and exploration of water bodies, prompting great interest in motion control for autonomous surface vessels (ASVs) [1]. Surface and underwater vessels motion control is nowadays an active research topic [2] given that accurate positioning and trajectory tracking are on the basis for autonomous vessel operations and are especially challenging due to under-actuation coupled with the nonlinearity of the dynamic models for vessels and external disturbances in the form of waves, wind and currents.

The common actuator configuration for an ASV consists of a stern propeller and a rudder surface providing a surge force and yaw moment, respectively. When the output is chosen at the position of the center of mass, the system is underactuated and non-minimum phase, i.e., it has unstable internal dynamics, resulting in a difficult control problem. The problem is inherently nonlinear as the linearization of the ship model around the desired position and orientation results in a system that is not controllable. Moreover, it can be shown that this problem cannot be asymptotically stabilized by any time-invariant state feedback law [3], [4].

Trajectory control can be achieved based on line-of-sight algorithms by controlling the yaw angle and the thrust force. The stability and performance of cross-talk error and proportional guidance laws were studied in [5], where their stability is also analyzed. Similarly, in [6] and [7] the guidance system is obtained through a waypoint guidance scheme based on line-of-sight projection algorithm and the speed controller is achieved through state feedback linearization. For this type of control algorithm, however, the reference trajectories are however limited to tracking waypoints or straight-lines. In [4] and [8] time-varying control laws are proposed to locally stabilize the desired equilibrium point. The former law only locally stabilizes the ship while the latter law achieves semiglobal practical stability for a simplified model of the ship.

A solution for a control objective of global practical stabilization of arbitrary reference trajectories was proposed in [9]. The solution is based on several nonlinear coordinate changes, the transverse function approach, a disturbance observer, Lyapunov direct method, and the backstepping technique, and successfully stabilizes fixed-points and non-admissible trajectories for underactuated ships. A cascade of proportional-derivative controllers and a nonlinear controller obtained through backstepping were developed and tested in [10]. Experimental results indicate that the backstepping controller is much more effective at tracking trajectories that involve large variations in speed and course angle. Trajectory tracking control for ships with unknown time-variant environmental disturbances was studied in [11]. An observer is constructed to provide an estimation of unknown disturbances and is applied to design a trajectory tracking robust controller through a vectorial backstepping technique. The tracking controller can force the ship to track an arbitrary reference trajectory and guarantee that all the signals of the closed-loop are globally uniformly ultimately bounded.

This paper presents a solution for the trajectory tracking of an underactuated autonomous surface vehicle subject to nonlinear drag and with coupled input forces and torques. The proposed controller is based on a double integrator controller and considers as output a fixed-point $\boldsymbol{\delta}$ in the body frame. With this fixed-point as output, as opposed to the center of mass, we are able to reduce the complexity of the controller and avoid the high noise and high accuracy dynamic models required for the standard backstepping approach for ASVs. The proposed solution is inspired by [12] but we choose to apply the $\boldsymbol{\delta}$ perturbation directly at the position level, instead of at the velocity error. This results in one fewer backstepping iteration compared to [12] (and two fewer iterations when compared with traditional backstepping) and

This work was partially supported by the projects MYRG2018-00198-FST and MYRG2016-00097-FST of the University of Macau, and by Fundação para a Ciência e a Tecnologia (FCT) through Project UID/EEA/50009/2019.

David Cabecinhas is with the Department of Electrical and Computer Engineering of the Faculty of Science and Technology of the University of Macau, Macao, China, and also with Institute for Systems and Robotics (ISR/IST), LARSyS, Portugal dcabecinhas@umac.mo

Carlos Silvestre is with the Department of Electrical and Computer Engineering of the Faculty of Science and Technology of the University of Macau, Macao, China, on leave from Instituto Superior Técnico/ University of Lisbon, 1049-001 Lisbon, Portugal csilvestre@umac.mo

attaches a physical meaning to the $\boldsymbol{\delta}$ parameter — it is the fixed-point, in the vessel's body frame, which is actually tracking the reference trajectory. Results obtained with an instrumented ASV reveals that the trajectories resulting from closed-loop application of the proposed controller are feasible and appropriate for the vessel's dynamics characteristics.

This paper is organized as follows. Section II presents a clear definition of the problem at hand. Section III introduces the surface vessel dynamic model and the controller design process is described in Section IV. The experimental setup is presented in Section V, the vehicle identification in Section VI and the results in Section VII. Finally, concluding remarks are featured in Section VIII.

II. Problem Statement

Consider a fixed inertial frame $\{I\}$ and a body frame $\{B\}$ attached to the boat's center of mass. The configuration of $\{B\}$ with respect to $\{I\}$ is given by the pair $(R, \mathbf{p}) = ({}^I_B R, {}^I\mathbf{p}_B)$. to the $x-y$ plane.

The trajectory tracking objective is to drive a fixed point in the boat body frame, $\boldsymbol{\delta}$, to follow a desired reference trajectory $\mathbf{p}_d(t) : \mathbb{R} \to \mathbb{R}^2$. The available actuations are the force provided by each motor propeller and the motor angle θ.

The orientation of the vehicle during the tracking maneuver is not *a priori* prescribed. Since the boat is underactuated, e.g. is not possible to generate a force with only lateral component, its final orientation will depend on the dynamics of the closed-loop system and the trajectory to be followed.

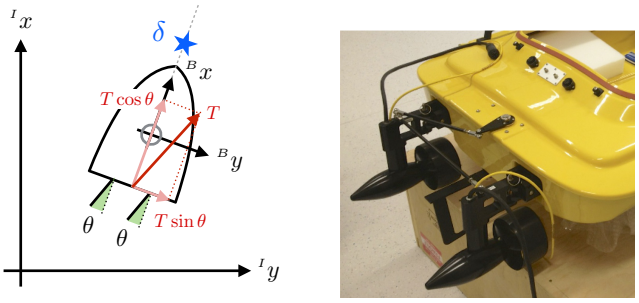

(a) Reference frame diagram. (b) Motor and propeller detail.

Fig. 1. Boat diagram and actuator detail.

III. Surface Vessel Dynamic Model

The surface vehicle is modeled as a rigid body dynamic system subject to linear and quadratic drag resulting in the dynamic model

$$\begin{aligned}
\dot{\mathbf{p}} &= R \begin{bmatrix} u \\ v \end{bmatrix}, \\
\dot{R} &= RSr, \\
\dot{u} &= m_{11}^{-1}(m_{22} vr + X_u u + X_{u|u|} u|u| + F_u), \\
\dot{v} &= m_{22}^{-1}(-m_{11} ur + Y_v v + F_v), \\
\dot{r} &= I_z^{-1}(N_r r + \tau),
\end{aligned} \tag{1}$$

where $\mathbf{v}_B = \begin{bmatrix} u & v \end{bmatrix}^T \in \mathbb{R}^2$ is the vessel's linear velocity, r is its angular velocity and the force and torque actuations are F_u, F_y, and τ. The matrices $R \in \mathrm{SO}(2)$ and S are defined as

$$R(\psi) = \begin{bmatrix} \cos\psi & -\sin(\psi) \\ \sin(\psi) & \cos(\psi) \end{bmatrix}, \quad S = \begin{bmatrix} 0 & -1 \\ 1 & 0 \end{bmatrix}.$$

where ψ is the vessel's heading. The remaining parameters are the mass, with added mass effects, in the surge and sway directions, m_{11} and m_{22}, the inertia I_z, the linear drag coefficients X_u, Y_v, N_r and the quadratic drag coefficient $X_{u|u|}$.

The force and torque actuations are functions of the individual motor thrusts f_p and f_s, corresponding to the impulse generated at the port and starboard motors, respectively, and the motor angle θ input as

$$\begin{aligned}
F_u &= (f_p + f_s)\cos\theta \\
F_v &= (f_p + f_s)\sin\theta \\
\tau &= (r_{px} f_p + r_{sx} f_s)\sin\theta - (r_{py} f_p + r_{sy} f_s)\cos\theta
\end{aligned}$$

where $\mathbf{r}_p = [r_{px}\ r_{py}]^T$ and $\mathbf{r}_s = [r_{sx}\ r_{sy}]^T$ are the locations of the port and starboard motors, respectively, with respect to the vehicle's center of mass. The boat has actuation redundancy in that the torque can be obtained with a trade-off between the motor differential and the rudder angle. To simplify the model and the controller design we consider zero differential motor actuation, corresponding to $f_p = f_s = \frac{1}{2}T$ and use the motor angle (as the vehicle does not have a rudder surface) as the only form of generating torque. The simplified inputs are then defined as

$$\begin{aligned}
F_u &= T\cos\theta \\
F_v &= T\sin\theta \\
\tau &= r_x T\sin\theta
\end{aligned}$$

where we used the equalities $r_{px} = r_{sx} = r_x$ and $r_{py} = -r_{sy}$.

IV. Controller Design

As stated in Section II, the control objective is to drive a fixed-point in the boat body-frame to the desired reference trajectory. The inertial position of the vehicle can be modeled as a double integrator system driven by the motor force which is commanded in magnitude and angle. This leads us to try a Lyapunov function appropriate for a double integrator and then use the available inputs to control it. In the sequel we will see how controlling a point that is not located at vessel's center of mass allows to simultaneously explore the torque input and the thrust force to drive the system to zero error without having to resort to further integrator backstepping iterations and higher-order derivatives.

Consider the tracking errors

$$\begin{aligned}
\mathbf{z}_1 &= \mathbf{p} - \mathbf{p}_d + R\boldsymbol{\delta} \\
\mathbf{z}_2 &= R\mathbf{v}_B - \dot{\mathbf{p}}_d + RS\boldsymbol{\delta} r
\end{aligned} \tag{2}$$

where $\mathbf{z}_2 = \dot{\mathbf{z}}_1$ and the tentative Lyapunov function

$$V = \tfrac{1}{2} K_1 \mathbf{z}_1^T \mathbf{z}_1 + \tfrac{1}{2} \mathbf{z}_2^T \mathbf{z}_2 + \beta \mathbf{z}_1^T \mathbf{z}_2.$$

The time derivative of V can be written as a controlled double-integrator system perturbed by the actual system dynamics as follows

$$\dot{V} = -W(\mathbf{z}_1, \mathbf{z}_2) + (\beta \mathbf{z}_1 + \mathbf{z}_2)^T (\dot{\mathbf{z}}_2 + \mathbf{u}^\star) \tag{3}$$

where

$$W(\mathbf{z}_1, \mathbf{z}_2) = K_1 \beta \mathbf{z}_1^T \mathbf{z}_1 + K_2 \beta \mathbf{z}_1^T \mathbf{z}_2 + (K_2 - \beta)\, \mathbf{z}_2^T \mathbf{z}_2$$

can be rendered positive definite with an appropriate choice of gains K_1, K_2, β, and

$$\mathbf{u}^\star = -K_1 \mathbf{z}_1 - K_2 \mathbf{z}_2$$

is the actuation that renders the nominal double integrator asymptotically stable. In (3), the term $\dot{\mathbf{z}}_2 + \mathbf{u}^\star$ can be seen as the actuation error between the actual system actuation, since $\dot{\mathbf{z}}_2$ includes the T and τ actuations, and the desired stabilizing actuation $\mathbf{u}^\star$.

Expanding $\dot{\mathbf{z}}_2$ and using the simplification $\boldsymbol{\delta} = \begin{bmatrix}\delta_x & 0\end{bmatrix}^T$ results in

$$\dot{V} = -W(\mathbf{z}_1, \mathbf{z}_2) + (\beta \mathbf{z}_1 + \mathbf{z}_2)^T R (TB \begin{bmatrix}\cos\theta \\ \sin\theta\end{bmatrix} + \mathbf{x}) \tag{4}$$

where we have highlighted the role of the actuations T and θ. The matrix B and vector $\mathbf{x}$ are defined as

$$B = \begin{bmatrix} m_{11}^{-1} & 0 \\ 0 & m_{22}^{-1} + \delta_x \mathbf{r}_x I_z^{-1} \end{bmatrix},$$

$$\mathbf{x} = rS\mathbf{v}_B + M^{-1} \begin{bmatrix} m_{22} vr + X_u u + X_{u|u|} u|u| \\ -m_{11} ur + Y_v v \end{bmatrix} - \boldsymbol{\delta} r^2 + N_r r I_z^{-1} S \boldsymbol{\delta} + R^T (K_1 \mathbf{z}_1 + K_2 \mathbf{z}_2 - \ddot{\mathbf{p}}_d).$$

The indefinite term in (4) can then be nullified, for an invertible matrix B, with actuations

$$T = \|\mathbf{u}\|,$$
$$\theta = \operatorname{atan2}(\mathbf{u}_2, \mathbf{u}_1),$$

and

$$\mathbf{u} = -B^{-1}\mathbf{x},$$

rendering the closed-loop Lyapunov time derivative negative definite. The arbitrary parameter δ_x can always be chosen so that B is invertible. The condition for invertibility of B is

$$\delta_x \neq \frac{I_z}{m_{22} \mathbf{r}_x}.$$

The convergence properties of the proposed solution for trajectory tracking are stated in Theorem 1.

Theorem 1: Consider the dynamic system (1), representing the kinematics and dynamics of a autonomous surface vessel and a desired trajectory $\mathbf{p}_d(t)$ of class at least C^2. Let $\boldsymbol{\delta} = \begin{bmatrix}\delta_x & 0\end{bmatrix}^T$ for an arbitrary δ_x satisfying

$$\delta_x \neq I_z m_{22}^{-1} \mathbf{r}_x^{-1}.$$

Let K_1 and K_2 be arbitrary positive control gains and β verify

$$0 < \beta < \min\left(\sqrt{K_1}, \frac{4K_1K_2}{4K_1 + K_2^2}\right). \tag{5}$$

Defining the position error states

$$\mathbf{z}_1 = \mathbf{p} - \mathbf{p}_d + R\boldsymbol{\delta},$$
$$\mathbf{z}_2 = R\mathbf{v}_B - \dot{\mathbf{p}}_d + RS\boldsymbol{\delta} r,$$

the auxiliary quantities

$$\mathbf{u} = -B^{-1}\mathbf{x},$$
$$B = \begin{bmatrix} m_{11}^{-1} & 0 \\ 0 & m_{22}^{-1} + \delta_x \mathbf{r}_x I_z^{-1} \end{bmatrix},$$
$$\mathbf{x} = rS\mathbf{v}_B + M^{-1} \begin{bmatrix} m_{22} vr + X_u u + X_{u|u|} u|u| \\ -m_{11} ur + Y_v v \end{bmatrix} - \boldsymbol{\delta} r^2 + N_r r I_z^{-1} S \boldsymbol{\delta} + R^T (K_1 \mathbf{z}_1 + K_2 \mathbf{z}_2 - \ddot{\mathbf{p}}_d),$$

and the plant inputs as

$$T = \|\mathbf{u}\|,$$
$$\theta = \operatorname{atan2}(\mathbf{u}_2, \mathbf{u}_1),$$

the origin of the error system is a global attractor and the target body-fixed point, whose inertial coordinates are $\mathbf{p} + R\boldsymbol{\delta}$, converges to the desired trajectory $\mathbf{p}_d(t)$.

Proof: The Lyapunov function

$$V = \tfrac{1}{2} K_1 \mathbf{z}_1^T \mathbf{z}_1 + \tfrac{1}{2} \mathbf{z}_2^T \mathbf{z}_2 + \beta \mathbf{z}_1^T \mathbf{z}_2$$

is positive definite for $\beta < \sqrt{K_1}$ and its closed-loop time derivative

$$\dot{V} = -K_1 \beta \mathbf{z}_1^T \mathbf{z}_1 - K_2 \beta \mathbf{z}_1^T \mathbf{z}_2 + (\beta - K_2)\, \mathbf{z}_2^T \mathbf{z}_2,$$

using the inputs in the theorem statement, is negative definite for β verifying (5). Using Lyapunov stability theory follows that both error states converge to zero with time. From the definition of $\mathbf{z}_1$ in (2), it follows that zero error corresponds to having the body-fixed point, defined by $\mathbf{p} + R\boldsymbol{\delta}$, track the reference trajectory $\mathbf{p}_d$. ■

The proposed controller is *simpler* in terms of dynamics than typical backstepping based controllers for surface vehicles. We only require up to the second derivative of the position error whereas for a backstepping controller four time derivatives are needed to surface the torque actuation. This dynamic simplicity comes at the expense of having to consider an off-centered point, $\boldsymbol{\delta}$, as the tracking goal instead of the center of mass of the vehicle.

A. Analysis of the Zero Dynamics

The zero error state is characterized by

$$\mathbf{z}_1 = 0,$$
$$\mathbf{z}_2 = 0,$$

from which it can be established that, in a zero error situation

$$\mathbf{p} = \mathbf{p}_d - R\boldsymbol{\delta},$$
$$\mathbf{v} = R^T \dot{\mathbf{p}}_d - RS\boldsymbol{\delta} r, \tag{6}$$

holds, resulting in immediate boundedness of both the position and the longitudinal velocity u, recalling that $\delta_y = 0$. It remains to be analyzed the boundedness of the lateral velocity v and r, which are related through (6). For the particular case where $\mathbf{p}_d(t)$ is a constant trajectory, we can

establish, based on the dynamics equations and the zero error condition that

$$\dot{r} = \frac{Y_v \delta_x r_x}{\delta_x m_{22} r_x + 1} r$$

which is stable if the coefficient on r is negative. Given that $Y_v < 0$, $\delta_x > 0$, $r_x < 0$, the stability condition reduces to $-\delta_x m_{22} r_x > 1$. In such case, the angular velocity converges to zero and the vehicle remains stationary in steady state with zero error.

V. Experimental Setup

The experiments were conducted with the DELMAC ASV, an instrumented OceanScience Q-Boat 1800P. The vehicle is depicted in Figure 2 and features twin orientable high-power out-drive motors with powerful brushless DC thrusters, capable of a 5 m/s maximum speed.

The vessel, originally a radio remote controlled vehicle, was instrumented with the necessary sensors and communication capabilities to transform it in an fully featured ASV. The vehicle position and velocity are determined using GPS Real Time Kinematic (RTK) positioning. A GPS receiver (Ashtech MB100) is used as shore station to send Real Time Correction Messages (RTCM) to the GPS unit installed in DELMAC via a radio Ethernet link. The other unit, installed onboard the ASV, receives the RTCM data and provides positioning data with centimeter-level accuracy. An onboard IMU (Inertial Measurement Unit) (Microstrain 3DM-GX3) based on a nine-axes solid state sensor outputs accurate acceleration, attitude and angular rates, and provides the heading and angular velocity feedback for implementing the proposed controller.

Communication between the shore station and the DELMAC ASV is performed using a set of two Ethernet radio modems (FreeWave HTPlus). These provide a reliable high data-rate and long distance link between the shore station and the ASV. The radio set transmits commands from the monitor console and RTCM data from the GPS base station to the ASV, and vehicle status data in the opposite direction to be displayed in the monitor console.

A low power consumption high-performance single-board-computer was installed on-board the ASV. This computer runs the mission control, navigation, and guidance and control systems. It is equipped with a solid-state disk to avoid disk damage due to the platform vibration, with interface boards to communicate with sensors and actuators, and Ethernet.

The vehicle and shore station operate in a ROS (Robot Operating System) environment integrating the sensors, controllers and communications. High-level commands and telemetry are transmitted between the vehicle and shore station using ROS messages.

VI. Identification

The surface vessel was originally remotely controlled and both inputs T and θ were specified as unitless parameters ranging from -1 to 1 which had to be mapped to their actual values, in Newton and angle, for a successful implementation of the proposed controller.

Fig. 2. The DELMAC autonomous surface vessel sailing on a pond at the University of Macau.

TABLE I
Identification of the vessel parameters

Parameter	Value
m_{11}	75.6
m_{22}	124.0
I_z	25.8
X_u	−32.6
$X_{u\|u\|}$	−20.2
Y_v	−49.8
N_r	−52.4

Experiments measuring the motor angle for different inputs determined that the mapping for the angle is linear and ranges in the interval [-60,60] deg. The thrust provided by the motors was identified through bollard pull tests where the pull force was measured for several input commands and a quadratic curve was fitted to the data. The outboard motors are controlled in linear rpm or current, resulting in a quadratic curve for the force. Results are presented in Figure 3.

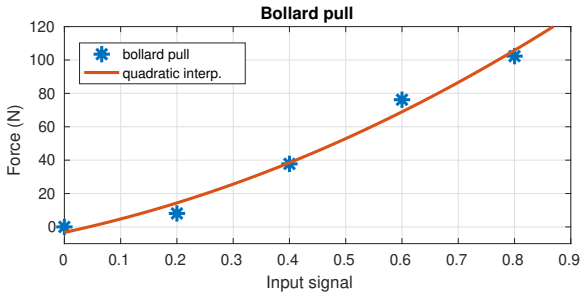

Fig. 3. Bollard pull tests at different motor inputs and quadratic interpolation

Having the exact inputs in SI units allows us to estimate the drag and added mass coefficients through a least squares fitting of the velocity measurement derivatives to the expressions in the vehicle model (1), for each of the unknown model parameters. The resulting parameter estimations are presented in Table I.

VII. Experimental Results

The proposed controller for the DELMAC autonomous surface vessel was tested experimentally at the University

TABLE II
CONTROLLER PARAMETERS

Parameter	Value
K_1	1.2
K_2	2.8
β	0.2
δ_x	2.0

of Macau by tracking two complex, varied, and aggressive trajectories: one a Lissajous curve, depicted in Fig. 4, and one figure eight, in Fig. 8, with varying velocity profiles.

The Lissajous curve desired trajectory and actual path taken by the delta point and the boat center of mass are shown in Fig. 4, and the trajectory tracking error for the delta point is isolated and presented in Fig. 5. For this maneuver the initial error was high, around 12 m, leading to a saturation of the thrust actuation until the vehicle caught up with the desired trajectory. Nonetheless, the proposed controller still stabilizes the vehicle and no adverse effect arises. With an eye on Fig. 10, we see that after a quick initial transient, where the boat rotates quickly to point in the direction of the desired position. The vehicle then follows an almost straight line, without much rudder actuation, until the desired trajectory is reached and tracked. This type of maneuver is consistent with how boats typically sail.

The tracking error in steady state is typically under 0.5 m. There are however occasional peaks of around 1.5 m error, correlated with higher speeds. This is probably indicative of inaccurate modeling of the propeller thrust at high rotations. Another possible explanation are the unmodeled varying dynamics of the boat as it hits waves and changes its submerged section. Notice that the tracking error is reasonable even though the trajectory is aggressive, in the sense that requires high rudder angles (with peaks of ± 40 deg) to track and also high thrust force. The aggressiveness of the trajectory is corroborated by the velocity plot where we can see that the lateral and longitudinal velocities are sometimes equal (17 and 35 s), corresponding to a sideslip angle of 45 deg. The longitudinal velocity ranges from 1 to 4 m/s throughout the trajectory, with the tracking error remaining low, showing that the proposed controller and dynamic models are well suited to the vehicle in study for a wide range of operating conditions.

An aerial view of the figure eight path is shown in Fig. 8 and the velocity profile for the vehicle is exposed in Fig. 11. The figure eight trajectory evolves in roughly the same area as the Lissajous trajectory but is less aggressive, in the sense that the longitudinal velocity only ranges from 1 to 3 m/s, resulting in smaller tracking errors. The typical steady state error is around 0.3 m while error peaks occasionally reach 0.9 m. However, high sideslip angles can still be noticed in Fig. 11 around 30 and 85 s.

As a final note, we would like the emphasize that despite the experimental tests being realized in a calm body of water, the high velocities (up to 5 m/s), lightness, and shallow hull of the vehicle make it so that even small ondulation, as seen in Fig. 2, has marked impact on the vehicle and leads to large fluctuations of the pitch angle as the vehicle sails. These pitch variations also change the submerged section of the vehicle, and consequently the added-mass and drag. Nonetheless, the proposed straightforward model and controller ensue good trajectory tracking results.

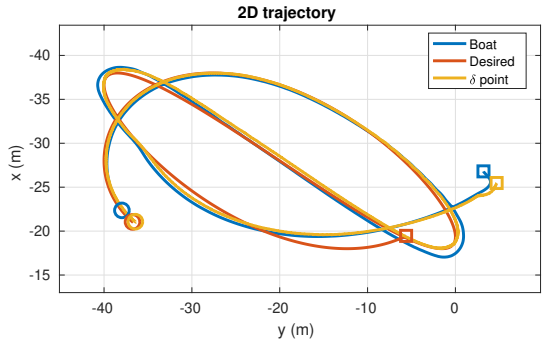

Fig. 4. Aerial view of the Lissajous trajectory followed by the boat, desired trajectory and trajectory followed by the controlled delta point. Trajectory starting points are marked with squares and end points are marked with circles.

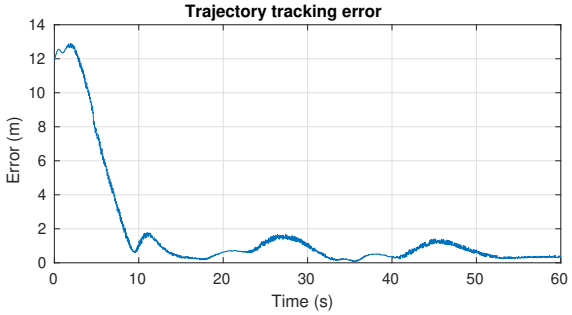

Fig. 5. Evolution of the tracking error along the trajectory. The controller manages to close the 12 m gap between the initial and the desired positions in less than 10 seconds. Once in steady state the error is typically under 0.5 m with occasional peaks of 1.5 m.

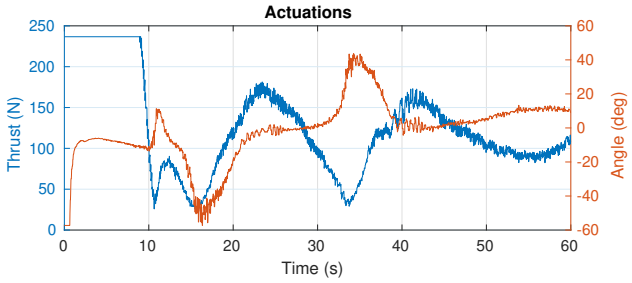

Fig. 6. Thrust and rudder actuations along the Lissajous trajectory. There is a quick initial turn of the boat, lasting one second, to align it with the current desired position accompanied by a maximum thrust actuation until the boat is close to the target trajectory.

VIII. CONCLUSIONS

This paper presented a nonlinear controller based on a double integrator system for trajectory tracking of an autonomous surface vessel. We used a fixed-point on the vessel body frame as position output and devised a simplified

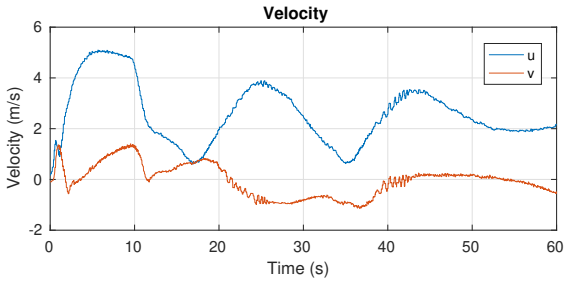

Fig. 7. Evolution of the body velocities while tracking the Lissajous trajectory. Notice the high sideslip reached at 17 s and 35 s when $|\mathbf{v}_{B_x}| \approx |\mathbf{v}_{B_y}| \approx 1$ m/s.

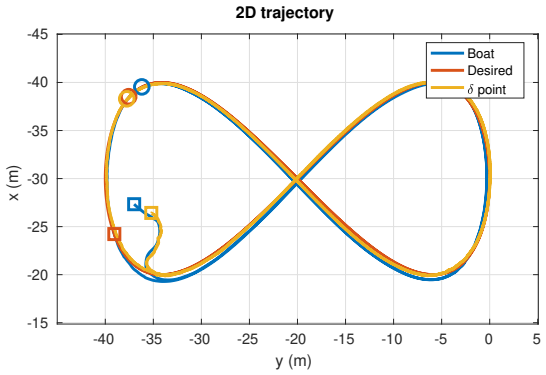

Fig. 8. Aerial view of the figure eight trajectory followed by the boat, desired trajectory and trajectory followed by the controlled delta point. Trajectory starting points are marked with squares and end points are marked with circles.

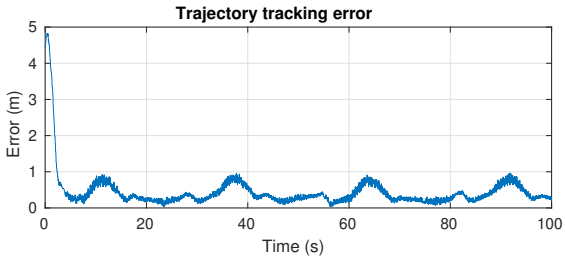

Fig. 9. Evolution of the tracking error along the figure eight trajectory. The controller manages to close the 5 m gap between the initial and the desired positions in less than 2.5 seconds. Once in steady state the error is typically under 0.3 m with occasional peaks of 0.9 m.

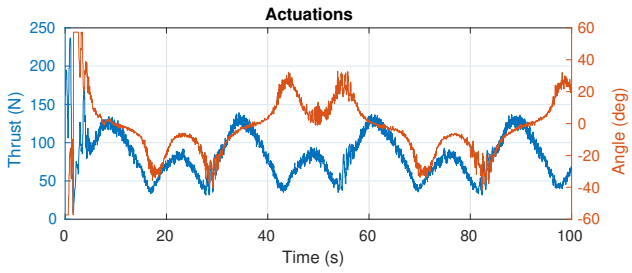

Fig. 10. Thrust and rudder actuations along the figure eight trajectory. There is a quick initial turn of the boat, lasting one second, to align it with the current desired position accompanied by a maximum thrust actuation until the boat is close to the target trajectory.

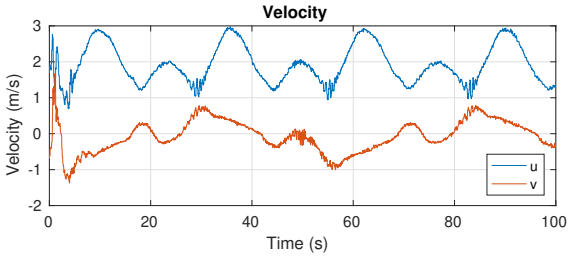

Fig. 11. Evolution of the body velocities while tracking the figure eight trajectory. Notice the high sideslip when $|\mathbf{v}_{B_y}| > |\mathbf{v}_{B_x}|$ around 5 s and when the longitudinal and lateral velocities are almost identical at 30 s and 85 s.

controller with only two states, as opposed to the four required in a more straightforward and naive backstepping approach. The resulting controller is dynamically simple and easy to implement, and does not require higher than second-order plant dynamics and reference trajectory derivatives. As the proposed approach requires fewer integrator backsteps than the backstepping approach, it mitigated typical backstepping problems such as noise amplification and the need for a highly accurate plant model. Experimental results in an instrumented autonomous surface vessel were presented to corroborate the performance and robustness of the proposed controller.

References

[1] J. Alves, P. Oliveira, R. Oliveira, A. Pascoal, M. Rufino, L. Sebastiao, and C. Silvestre, "Vehicle and mission control of the delfim autonomous surface craft," in *2006 14th Mediterranean Conference on Control and Automation*, June 2006, pp. 1–6.

[2] K. D. Do and J. Pan, *Control of Ships and Underwater Vehicles: Design for Underactuated and Nonlinear Marine Systems*. Springer Science & Business Media, Aug. 2009, google-Books-ID: OSC9L4X801sC.

[3] R. W. Brockett, "Asymptotic stability and feedback stabilization," in *Differential Geometric Control Theory*. Birkhauser, 1983, pp. 181–191.

[4] K. Y. Pettersen and O. Egeland, "Exponential stabilization of an underactuated surface vessel," in *Proceedings of 35th IEEE Conference on Decision and Control*, vol. 1, Dec. 1996, pp. 967–972 vol.1.

[5] F. A. Papoulias, "Cross Track Error and Proportional Turning Rate Guidance of Marine Vehicles," *Journal of Ship Research*, vol. 38, pp. 123–132, 1994.

[6] T. I. Fossen, M. Breivik, and R. Skjetne, "Line-of-sight path following of underactuated marine craft," *IFAC Proceedings Volumes*, vol. 36, no. 21, pp. 211–216, Sept. 2003.

[7] L. Moreira, T. I. Fossen, and C. G. Soares, "Path following control system for a tanker ship model," *Ocean Engineering*, vol. 34, no. 14, pp. 2074 – 2085, 2007.

[8] K. Y. Pettersen and H. Nijmeijer, "Global Practical Stabilization and Tracking for an Underactuated Ship - A Combined Averaging and Backstepping Approach," *IFAC Proceedings Volumes*, vol. 31, no. 18, pp. 59–64, July 1998.

[9] K. D. Do, "Practical control of underactuated ships," *Ocean Engineering*, vol. 37, no. 13, pp. 1111–1119, Sept. 2010.

[10] C. Sonnenburg and C. A. Woolsey, "An experimental comparison of two USV trajectory tracking control laws," in *2012 Oceans*, Oct. 2012, pp. 1–10.

[11] Y. Yang, J. Du, H. Liu, C. Guo, and A. Abraham, "A Trajectory Tracking Robust Controller of Surface Vessels With Disturbance Uncertainties," *IEEE Transactions on Control Systems Technology*, vol. 22, no. 4, pp. 1511–1518, July 2014.

[12] A. P. Aguiar, L. Cremean, and J. P. Hespanha, "Position tracking for a nonlinear underactuated hovercraft: controller design and experimental results," in *42nd IEEE International Conference on Decision and Control (IEEE Cat. No.03CH37475)*, vol. 4, Dec. 2003, pp. 3858–3863 vol.4.